# POLYMORPHIC TRANSFORMATION OF TITANIUM DIOXIDE CAUSED BY HEAT TREATMENT OF PROTONIC LEPIDOCROCITE TITANATE

**Hari Sutrisno* and Sunarto**

*Department of Chemical Education, Faculty of Mathematics and Natural Science, Yogyakarta State University (YSU), Kampus Karangmalang, Yogyakarta 55281, Indonesia*

*Received March 15, 2010; Accepted May 6, 2010*

## ABSTRACT

*The polymorphic phases of titanium dioxide were successfully prepared by heat treatments of protonic lepidocrocite titanate, $H_{0.54}Ti_{1.865}\square_{0.135}O_4{\cdot}0.5H_2O$ at various temperatures. The prepared powders were characterized with EDX (Energy Dispersive X-ray), Scanning Electron Microscopy (SEM), X-rays Diffractometer (XRD), Raman Spectroscopy, and High Resolution Transmission Electron Microscopy (HRTEM). The effect of calcination temperature on the phase structure and morphology of the heated samples was investigated. The research indicated that the protonic titanate, $H_{0.54}Ti_{1.865}\square_{0.135}O_4{\cdot}0.5H_2O$ ($\square$ = vacancy), lost the interlayer water by being heated up to 200 °C to produce a dehydrated phase, $H_{0.54}Ti_{1.865}\square_{0.135}O_4$. Above 300 °C, the dehydrated phase, $H_{0.54}Ti_{1.865}\square_{0.135}O_4$, completely transformed to $TiO_2$(B) and anatase was obtained as pure phase at 600 °C. The phase transformed as the following process: $H_{0.54}Ti_{1.865}\square_{0.135}O_4{\cdot}0.5H_2O \rightarrow H_{0.54}Ti_{1.865}\square_{0.135}O_4{\cdot}0.25H_2 \rightarrow H_{0.54}Ti_{1.865}\square_{0.135}O_4 \rightarrow TiO_2$(B) $\rightarrow$ $TiO_2$-anatase.*

**Keywords**: *layered compound, titanium dioxide, lepidocrocite, phase transformation, heat treatment*

## INTRODUCTION

Titanium dioxide ($TiO_2$) is considered to be one of the most promising materials due to its excellent physicochemical stability, high oxidation affinity, mechanical hardness, superior photo-reactivity and novel optoelectronic properties. It is widely used as white pigment in paints, cosmetics, photoelectrochemistry and catalyst carrier in industry [1]. Titanium dioxide as an n-type semiconductor with a wide energy band gap is well-known for its potential applications in the field of photovoltaic devices [2-6], superhydrophilic and light-induced amphiphilic surfaces [7-10] and antibacterial applications [11-13]. It can be also applied in heterogenous photocatalysis [14]. The photocatalytic activity of $TiO_2$ is markedly influenced by the microstructure, polymorphic phases, particle shape, crystallite size, crystallinity, and specific surface area. $TiO_2$ nanoparticles show high photocatalytic activities because they have a large surface area per unit mass and volume, and hence facilitate the diffusion of excited electrons and holes towards the surface before their recombination. This process involves a large variety of reactions, for example, partial or total oxidation, dehydrogenation, hydrogen transfer, metal deposition, water detoxification, or gaseous pollutant removal [15-19].

Titanium dioxide has eleven polymorphic phases: anatase (tetragonal, $I4_1/amd$) [20], rutile (tetragonal, $P4_2/mnm$) [21-22], brookite (orthorombic, *Pbca*) [23], $TiO_2$(B) (monoclinic, $C2/m$) [24], $TiO_2$(H)-hollandite (tetragonal, $I4/m$) [25], $TiO_2$(R)-ramsdellite (orthorombic, *Pbnm*) [26], $TiO_2$-columbite type $\alpha$-$PbO_2$ ($TiO_2$-II) (orthorombic, *Pbnm*) [27-28], $TiO_2$ baddeleyite type ($TiO_2$-MI) (monoclinic, $P2_1/c$) [29-30], $TiO_2$-orthorombik ($TiO_2$-OI) (ortorombik, *Pbca*) [31], $TiO_2$ fluorite type $CaF_2$ (cubic, *Fm3m*) [32] dan $TiO_2$ cotunnite type (orthorombic, *Pnma*) [33]. Rutile is a stable phase, while anatase and brookite are metastable and will be transformed into a thermodynamically most stable rutile phase at higher temperature after thermal treatment. The low temperature anatase phase is irreversibly transformed to rutile phase on heat treatment above 450 °C. The transformation from anatase to rutile is metastable-to-stable transformation and there is no equilibrium temperature of the transformation. The transformation temperature range varies from 400 °C to 1200 °C, depending on the grain size, presence of impurities, dopants, precursor material and synthesis method [34].

The photocatalytic performance of $TiO_2$ can be optimized by microstructural and macrostructural control on the morphology of the material because of the intimately morphology-dependent characteristic of the photocatalytic properties. It is interesting and necessary to investigate the process of the $TiO_2$ phase transformation, both from a scientific and from a technological point of view. Nanostructured $TiO_2$ materials can be prepared by dry and wet processes. In this work, the $TiO_2$ polymorphic phases are prepared

* Corresponding author. Tel/Fax : +62-274-548403
Email address : sutrisnohari@uny.ac.id

by the heat treatments of lepidocrocite-structure type titanate, and the phase transformation is investigated by ex situ XRD and FT-Raman. The effects of heat treatments on the $TiO_2$ polymorphic were also investigated in detail.

## EXPERIMENTAL SECTION

### Materials

Cesium titanate for this research was prepared from pure-grade: $Cs_2CO_3$ (Merck, 99.99%) and $TiO_2$-anatase (Millenium, 98.5%). $H^+$-exchange reactions for $Cs_xTi_{2-x/4}\square_{x/4}O_4$ were carried out by suspending the powder in an aqueous 1 mol $dm^{-3}$ HCl (Aldrich) solution HCl (Aldrich). The protonic titanate was washed by distilled water.

### Instrumentation

The structures of the prepared powders were collected using a Bruker D8 Advance diffractometer, operating in the Bragg-Brentano configuration using Cu Kα radiation ($\lambda$ = 1.5406 Å) in a step-scan mode (step interval 0.03° in 2$\theta$) over an angular range 5-80°. The accelerating voltage and the applied current were 40 kV and 30 mA, respectively. Lattice parameters were determined by a least-squarest procedure with a U-fit program [36].

The degree of $H^+$ exchange was determined by an EDX (Energy Dispersive X-ray) instrument equipped with a PGT X-ray analysis probe attached to JEOL 5800LV SEM with a conventional tungsten electron source operating at 10 keV.

HRTEM (High Resolution Transmission Electron Microscopy) analyses were conducted to investigate the morphologies and microstructures of the obtained powders with a Hitachi HNAR-9000 transmission electron microscope using 300 kV accelerating voltage.

Raman studies were performed on a Bruker RFS100 equipped with a radiation of 1064 nm from an Nd-YAG laser, which allows one to focus a sample area with a diameter less than 1 mm.

### Procedure

The cesium titanate, $Cs_xTi_{2-x/4}\square_{x/4}O_4$ (□ = vacancy) was prepared by a conventional heating a mixture of $Cs_2CO_3$ (Merck, 99.99%) and $TiO_2$-anatase (Millenium, 98.5%). An intimate mixture where the molar ratio of $Cs_2CO_3/TiO_2$ = 1/5.3 was placed in a Pt crucible and was heated at 800 °C for 1 h to be decarbonated. The mixture was ground and then allowed to 2 cycles of heating at 800 °C for 20 h [35]. The obtained powder (cesium titanate) was washed by distilled water, filtered in the vacuum and dried at 70 °C for 24 h. $H^+$-exchange reactions for $Cs_xTi_{2-x/4}\square_{x/4}O_4$ were carried out by suspending the powder in an aqueous 1 mol $dm^{-3}$ HCl (Aldrich) solution at room temperature for 5 days. The HCl concentration was 1 mol $dm^{-3}$ and the solution-to-solid ratio was 100 $cm^3\ g^{-1}$. During the proton exchange reaction, the HCl solution was replaced with a fresh one every day. The solution was filtered and washed by distilled water. The washing treatment was repeated until the washing water showed pH ~ 5. After the washing treatment, they were filtered and subsequently dried at 70 °C for 24 h in an oven. Finally, the hydrogen titanate, $H_xTi_{2-x/4}\square_{x/4}O_4$, was heated for 2 h at 100, 200, 300, 400, 500 and 600 °C, respectively.

## RESULT AND DISCUSSION

### Synthesis of Cesium Titanate and Protonic Titanate

The Cs/Ti and Ti/O ratio deduced from EDX on cesium and hydrogen titanate lead to the formula $Cs_{0.54}Ti_{1.865}\square_{0.135}O_4{\cdot}0.17H_2O$ (Fig. 1) and $H_{0.54}Ti_{1.865}\square_{0.135}O_4{\cdot}0.5H_2O$ respectively (Fig. 2). The XRD pattern

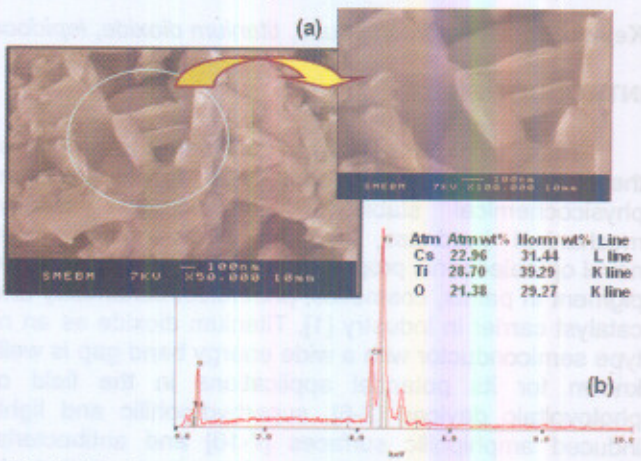


**Fig 1**. (a). SEM image and (b). EDX of sesium titanate

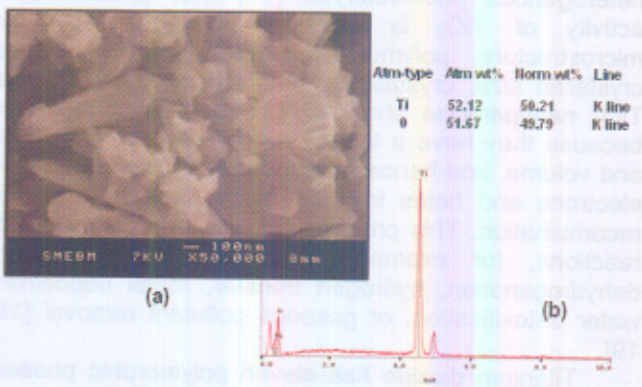


**Fig 2**. (a). SEM image and (b). EDX of protonic titanate

**Table 1.** Lattice parameters, symmetries, and chemical formulas of the layered titanates

| Samples | a (Å) | b (Å) | c (Å) | Symmetry | Chemical formula |
|---|---|---|---|---|---|
| Cesium titanate | 3.8097 | 17.6436 | 2.9638 | orthorhombic | $Cs_{0.54}Ti_{1.865}O_4{\cdot}0.17H_2O$ |
| Protonic titanate | 3.6523 | 15.7075 | 3.0994 | orthorhombic | $H_{0.54}Ti_{1.865}O_4{\cdot}0.5H_2O$ |

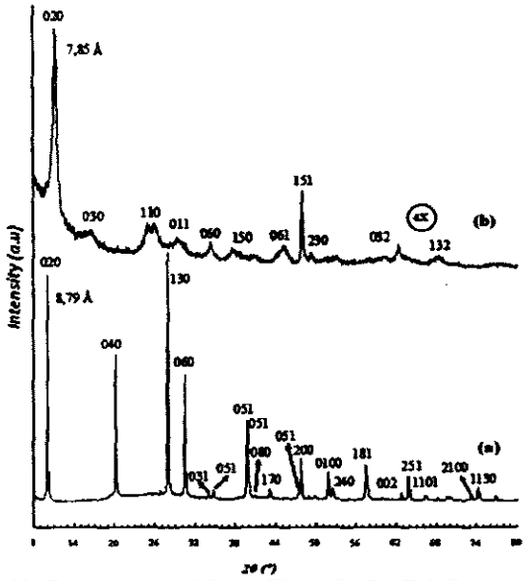


**Fig 3.** XRD patterns of $Cs_{0.54}Ti_{1.865}O_4{\cdot}0.17H_2O$ (a) before and (b) after treatment with acid chloride

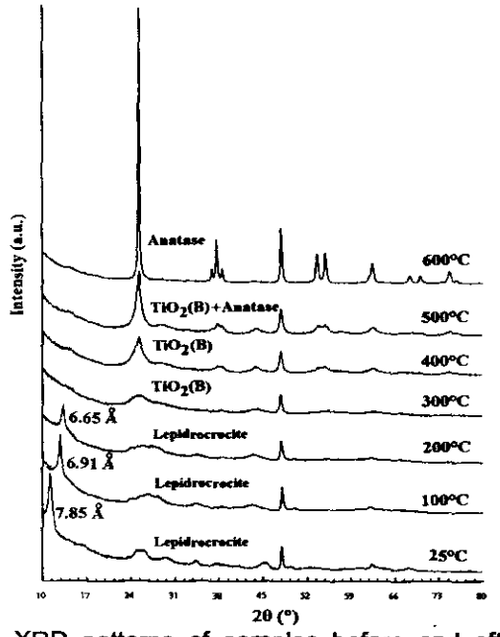


**Fig 4.** XRD patterns of samples before and after the heat treatment of $H_{0.54}Ti_{1.865}O_4{\cdot}0.5H_2O$

of the layered cesium titanate shows the lepidocrocite structure with orthorhombic symmetry as well established. The powder XRD pattern of the $Cs_{0.54}Ti_{1.865}\square_{0.135}O_4{\cdot}0.17H_2O$ is shown in Fig. 3, together with that of the proton-exchanged form $H_{0.54}Ti_{1.865}\square_{0.135}O_4{\cdot}0.5H_2O$, and the lattice parameters obtained from the least-squares fitting analyses are summarized in Table 1. Upon acid-treatment, the (020) reflection of the layered cesium titanate (d = 8.79 Å) is shifted toward a higher angle, indicating lattice contraction due to intercalation of water molecules into the interlayer space of the protonic titanate (d = 7.85 Å).

**Phases Transformation of protonic titanate**

Transformation from $H_{0.54}Ti_{1.865}\square_{0.135}O_4{\cdot}0.5H_2O$ to $TiO_2$-anatase may occur through several steps under the heat treatments. The phase transformation of the products was studied by X-ray diffractometer (XRD) and Raman spectroscopy. Fig. 4 shows the XRD patterns of $H_{0.54}Ti_{1.865}\square_{0.135}O_4{\cdot}0.5H_2O$ calcined at different temperature: 100, 200, 300, 400, 500 and 600 °C. Calcinations' at 100 °C resulted in a steady decrease of the peaks intensity and finally contraction of the basal distance from 7.85 to 6.65 Å. The titanate, $H_{0.54}Ti_{1.865}\square_{0.135}O_4{\cdot}0.5H_2O$, lost the interlayer water by being heated up to 200°C to produce a dehydrated phase, $H_{0.54}Ti_{1.865}\square_{0.135}O_4$, the interlayer spacing of which was 6.65 Å [35,37]. The layered structure was completely collapsed between 300 °C and 600 °C. Above 300 °C, the dehydrated phase, $H_{0.54}Ti_{1.865}\square_{0.135}O_4$, completely transformed to $TiO_2$(B) [38] and anatase was obtained as pure phase at 600 °C [39].

**Raman Spectra**

Raman spectra were recorded to identify the phase composition. A comparison of Raman spectroscopy with X-ray diffraction can be used to estimate the difference between the compositions of phases $TiO_2$. Fig. 5 shows the Raman spectra of the protonic titanate before and after the heat treatment at various temperatures for 2 h. Nine Raman bands were observed for the protonic titanate before and after the heat treatments at 100 °C and at 200 °C (Fig. 5a - 5c): 145, 195, 266, 341, 448, 614, 645, 703 and 935 $cm^{-1}$, which was confirmed as being the lepidocrocite type titanate. The number of observed modes agrees fairly well with the space group theoretical analysis of lepidocrocite titanate, which yields nine ($3A_g$ + $3B_{2g}$ + $3B_{1g}$) modes. Their peak position and profile are very similar to those of protonic lepidocrocite titanate [40-41],

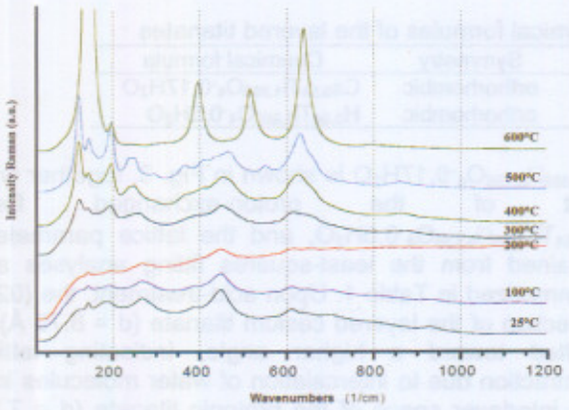


**Fig 5.** Raman spectra of samples before and after the heat treatment of $H_{0.54}Ti_{1.865}O_4.0.5H_2O$

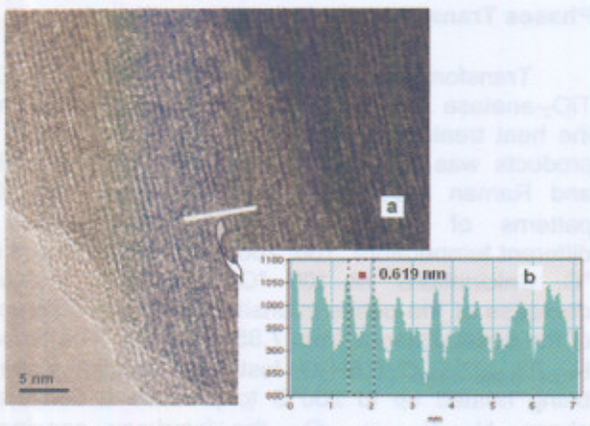


**Fig 6.** (a). HRTEM image and (b). electron diffraction spectra of $TiO_2$(B) (*the powder obtained by heat treatment of protonic lepidocrocite titanate for 2 h at 300 °C*)

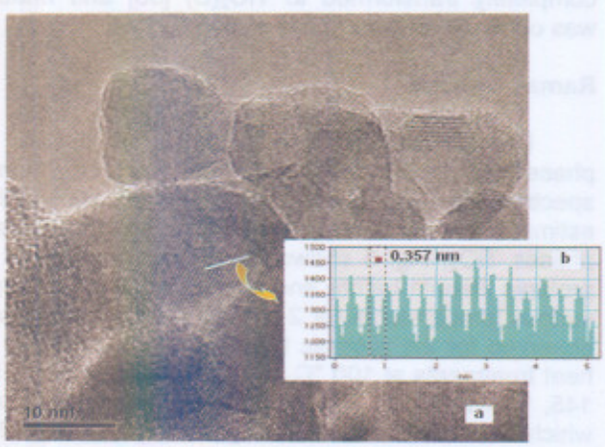


**Fig 7.** (a). HRTEM image and (b). electron diffraction spectra of anatase (*the powder obtained by the heat treatment of protonic lepidocrocite titanate for 2 h at 600 °C*)

in accordance with the XRD result previously discussed. The Raman spectra of the samples obtained by the heat treatments of protonic titanate at 300, 400 and 500 °C respectively are shown in Fig. 5d - 5f. Twelve peaks at 123, 145, 198, 239, 251, 295, 350, 407, 471, 552, 632 and 660 $cm^{-1}$ can be assigned to $TiO_2$(B). These observations are similar to those reported in the literature [42]. In the Raman spectra of the heat treated samples at 600 °C, it can be observed several characteristic peaks of $TiO_2$ anatase phase at 144, 195, 398, 516 and 640 $cm^{-1}$. Based on the factor group analysis, the 398 $cm^{-1}$ peak is assigned to the $B_{1g}$ mode ($v_4$); 640 $cm^{-1}$ peak can be attributed to the $E_g$ mode ($v_1$); 516 $cm^{-1}$ peak can be attributed to the $A_{1g} + B_{1g}$ modes ($v_2$+$v_3$). The peaks at 195 and 144 $cm^{-1}$ are assigned to the $E_g$ modes represented by $v5$ and $v6$ [43].

### High Resolution Transmission Electron Microscopy

HRTEM was used to investigate the exact microstructure of $TiO_2$ obtained after the heat treatments of protonic lepidocrocite titanate for 2 h at 300 and at 600 °C as shown in Fig. 6 and 7 respectively. In Fig. 6, the fringe spacing of 0.619 nm is very close to the fringe spacing of the (001) planes of $TiO_2$(B) [44]. The HRTEM image of the heat treated sample at 600 °C (Fig. 7) shows spherical particles with an average size of approximately 10-50 nm. The well-resolved lattice fringes allow an accurate measurement of crystallographic spacing and identification of the observed crystallites. The measured fringe spacing of 0.357 nm matches well with the distance between the (101) crystal planes of $TiO_2$-anatase [45].

### Transformation Mechanism of Protonic Titanate Caused by Heat Treatment

X-ray diffraction and Raman data of $TiO_2$ phases obtained by the heat treatment showed that there should be three-step phase transformation under ex-situ condensation process as follows:

$H_{0.54}Ti_{1.865}\square_{0.135}O_4{\cdot}0.5H_2O \rightarrow H_{0.54}Ti_{1.865}\square_{0.135}O_4{\cdot}0.25H_2O$
$\rightarrow H_{0.54}Ti_{1.865}\square_{0.135}O_4$

$H_{0.54}Ti_{1.865}\square_{0.135}O_4 \rightarrow 1.865\ TiO_2$(B)

$TiO_2$(B) $\rightarrow$ $TiO_2$-anatase

The corresponding structural transformation is illustrated in Fig. 8. Firstly, $H_{0.54}Ti_{1.865}\square_{0.135}O_4{\cdot}0.5H_2O$ transforms into $H_{0.54}Ti_{1.865}\square_{0.135}O_4$ through dehydration. After annealing at 300 °C, dehydration and condensation of the layered protonic lepidocrocite titanate convert it into $TiO_2$(B) with growth direction [010] axis. At last, $TiO_2$(B) transforms into $TiO_2$-anatase without dehydration. The double octahedral ribbons could split or shear into single $2TiO_6$ octahedral ribbons

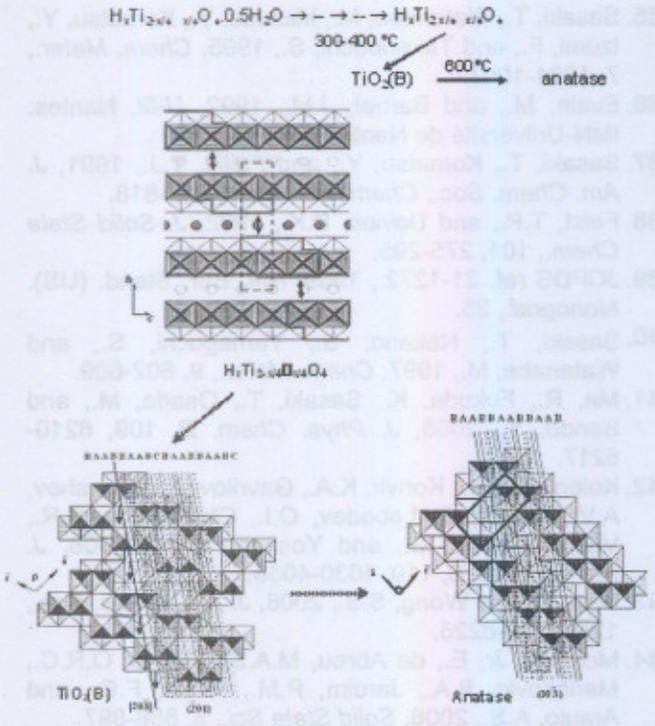


**Fig 8.** Mechanism of the transformation phases of protonic titanate to polymorphic $TiO_2$

and shift by each other to form $TiO_2$-anatase. The detailed mechanism for the latter phase transformation has been widely studied by Brohan et al. [46]. The transformation from $TiO_2$(B) to anatase was explained by the shear of $(\bar{2}01)$-$TiO_2$(B) plane to form $(10\bar{3})$-anatase plane, along with the $(\bar{2}01)$-$TiO_2$(B) direction.

## CONCLUSION

The $TiO_2$ polymorphic phases were obtained by the ex-situ condensation of protonic lepidocrocite titanate. The phase transformed as the following process: $H_{0.54}Ti_{1.865}\square_{0.135}O_4 \cdot 0.5H_2O \rightarrow H_{0.54}Ti_{1.865}\square_{0.135}O_4 \cdot 0.25H_2O \rightarrow H_{0.54}Ti_{1.865}\square_{0.135}O_4 \rightarrow TiO_2$(B) $\rightarrow$ $TiO_2$-anatase. The protonic lepidocrocite titanate convert it into $TiO_2$(B) by heat treatment at 300-400 °C and then $TiO_2$-anatase structures at 600 °C.

## ACKNOWLEDGEMENT

The authors wish to thank Dr. Luc Brohan (CESES Group, Laboratoire IMN-Jean Rouxel, Université de Nantes, France). This work is supported by the Ministry of National Education of Indonesia through Fund Research Project No. 018/SP2H/PP/DP2M/III/2008.

## REFERENCES

1. Carp, O., Huisman, C.L., and Reller, A., 2004, *Progr. Solid State Chem.*, 32, 33-177.
2. Grätzel, M., 2004, *J. Photochem. Photobiol., A*, 164, 3-164.
3. Grätzel, M., 2005, *Inorg. Chem.*, 44, 6841-6851.
4. O'regan, B., and Grätzel, M., 1991, *Nature*, 353, 737-740.
5. Bach, U., Lupo, D., Compte, P., Moser, J.E., Weissörtel, F., Salbeck, J., Spreitzer, H., and Grätzel, M., 1998, *Nature*, 395, 583-585.
6. Tan, B. and Wu, Y., 2006, *J. Phys. Chem. B*, 110, 15932-15938.
7. Ashkarran, A.A., and Mohammadizadeh, M.R., 2008, *Mater. Res. Bull.*, 43, 522-530.
8. Masuda, Y., and Kato, K., 2008, *Chem. Mater.*, 20, 1057-1063.
9. Wang, R., Hashimoto, K., Fujishima, A., Chikuni, M., Kojima, E., Kitamura, A., Shimohigoshi, M., and Watanabe, T., 1997, *Nature*, 388, 431-433.
10. Wang, R., Hashimoto, K., Fujishima, A., Chikuni, M., Kojima, E., Kitamura, A., Shimohigoshi, M., and Watanabe, T., 1998, *Adv. Mater.*, 10, 135-139.
11. Shah, M.S.A.S., Nag, M., Kalagara, T., Singh, S., and Manorama, S.V., 2008, *Chem. Mater.*, 20, 2455-2459.
12. Huang, Z., Maness, P.C., Blake, D.M., Wolfrum, E.J., Smolinski, S., and Jacoby, W.A., 2000, *J. Photochem. Photobiol., A*, 130, 163-170.
13. Maness, P.C., Smolinski, S., Blake, D.M., Huang, Z., Wolfrum, E.J., and Jacoby, W.A., 1999, *Appl. Environ. Microbiol.*, 65(9), 4094-4098.
14. Thompson, T.L., and Yates Jr., J.T., 2006, *Chem. Rev.*, 106, 4428-4453.
15. Lu, C-H., Wu, W-H., and Kale, R.B., 2008, *J. Hazard. Mater.*, 154, 649-654.
16. Aizawa, M., Morikawa, Y., Namai, Y., Morikawa, H., and Iwasawa, Y., 2005, *J. Phys. Chem. B*, 109, 18831-18837.
17. Rice, C.V. and Raftery, D., 1999, *J. Chem. Soc., Chem. Commun.*, 895-896.
18. Dai, Q., Zhang, Z., He, N., Li, P., and Yuan, C., 1999, *Mater. Sci. Eng.*, C, 8-9, 417-423.
19. Awati, P.S., Awate, S.V., Shah, P.P., and Ramaswamy, V., 2003, *Catal. Commun.*, 4, 393-398.
20. Weirich, T. E., Winterer, M., Seifried, S., Hahn, H. and Fuess, H., 2000, *Ultramicroscopy*, 81, 3-4, 263-270.
21. Abrahams, S.C., and Bernstein, J.L., 1971, *J. Chem. Phys.*, 55, 3206-3211.
22. Swope, R.J., Smyth, J.R., and Larson, A.C., 1995, *Am. Mineral.*, 80, 448-453.

23. Baur, W.H., 1961, *Acta Cryst.*, 14, 214-216.
24. Marchand, R., Brohan, L., and Tournoux, M., 1980, *Mater. Res. Bull.*, 15, 1129-1133.
25. Latroche, M., Brohan, L., Marchand, R. and Tournoux, M., 1989, *J. Solid State Chem.*, 31, 78-82.
26. Akimoto, J., Gotoh, Y., Osawa, Y., Nonose, N., Kumagai, T., Aoki, K., and Takei, H., 1994, *J. Solid State Chem.*, 113, 27-36.
27. Simons, P.Y., and Dachille, F., 1967, *Acta Cryst.*, 23, 334-336.
28. Grey, I.E., Li, C., Madsen, I.C., and Braunshausen, G., 1988, *Mater. Res. Bull.*, 23, 5, 743-753.
29. Kuo, M.Y., Chen, C.L., Hua, C.Y., Yang, H.C., and Shen, P., 2005, *J. Phys. Chem. B*, 109, 8693-8700.
30. Sato, H., Endo, S., Sugiyama, M., Kikegawa, T., Shimomura, O., and Kusaba, K., 1991, *Science*, 251, 4995, 786-788.
31. Dubrovinskaia, N.A., Dubrovinsky, L.S., Ahuja, R., Prokopenko, V.B., Dmitriev, V., Weber, H.P., Osorio-Guillen, J.M., and Johansson, B., 2001, *Phys. Rev. Lett.*, 87, 27, 275501-275504.
32. Mattesini, M., De Almeida, J., Dubrovinsky, L.S, Dubrovinskaia, N.A., Johansson, B., and Ahuja, R., 2004, *Phy. Rev. B*, 70, 21, 212101-(1)-212101-(4).
33. Dubrovinsky, L.S., Durovinskaia, N.A., Swamy, V., Muscat, J., Horrison, N.M., Ahuja, R., Holm, B., and Johansson, B., 2001, *Nature*, 410, 653-658.
34. Hirano, M., Nakahara, C., Ota, K., Tanaike, O., and Inagaki, M., 2003, *J. Solid State Chem.*, 170, 39-45.
35. Sasaki, T., Watanabe, M., Michiue, Y., Komatsu, Y., Izumi, F., and Takenouchi, S., 1995, *Chem. Mater.*, 7, 1001-1007.
36. Evain, M., and Barbet, J.M., 1992, *U-fit*, Nantes: IMN-Université de Nantes, France.
37. Sasaki, T., Komatsu, Y., and Fujiki, Y.J., 1991, *J. Am. Chem. Soc., Chem. Commun.*, 817-818.
38. Feist, T.P., and Davies, P.K., 1992, *J. Solid State Chem.*, 101, 275-295.
39. JCPDS ref. 21-1272., 1969, Nat. Bur. Stand. (US). *Monograf.*, 25.
40. Sasaki, T., Nakano, S., Yamaguchi, S., and Watanabe, M., 1997, *Chem. Mater.*, 9, 602-609.
41. Ma, R., Fukuda, K., Sasaki, T., Osada, M., and Bando, Y., 2005, *J. Phys. Chem. B*, 109, 6210-6217.
42. Kolen'ko, Y.V., Konvir, K.A., Gavrilov, A.I., Garshev, A.V., Frantti, J., Lebedev, O.I., Churagulov, B.R., Van Tendeloo, G., and Yoshimura, M., 2006, *J. Phys. Chem. B*, 110, 4030-4038.
43. Mao, L., and Wong, S.S., 2006, *J. Am. Chem. Soc.*, 128, 8217-8225.
44. Morgado Jr, E., de Abreu, M.A.S., Pravia, O.R.C., Marinkovic, B.A., Jardim, P.M., Rizzo, F.C., and Araujo, A.S., 2006, *Solid State Sci.*, 8, 888-897.
45. Wen, P., Itoh, H., Tang, W., and Feng, Q., 2007, *Langmuir*, 23, 11782-11790.
46. Brohan, L., Verbaere, A., and Tournoux, M., 1982, *Mater. Res. Bull.*, 17, 355-364.